Design and experiment on the air-blowing and vibrating supply seed tray for precision seeders

Zhiqiao Zhang, Jin Chen*, Yaoming Li, Zhuohuai Guan, Caiqi Liao, Xiangshan Qiao

(*College of Mechanical Engineering, Jiangsu University, Zhenjiang 212013, Jiangsu, China*)

Abstract: Vacuum-vibration precision seeding technology is a crucial technology that affects the industrialization process of super rice plug seedlings. To solve the problems that the vibrating supply seed tray structure in a vacuum-vibration precision seeder caused the vibration of the whole machine and the decline of the seeding eligible rate under high frequency and large amplitude vibration, it is important to design a new supply seed tray structure. This research proposed a method to make the seeds "boiling" under the combined effect of air blowing and vibration, and designed the air-blowing and vibrating supply seed tray structure. FLUENT was used to analyze fluid motion inside the supply seed tray and optimize the structure parameters of the supply seed tray. The maximum airflow velocity was determined when the inlet air pressure was 22 kPa, the number of air inlets was 2, and the diameter of the holes at the bottom of the supply seed tray was 2 mm. Comparative experiments were carried out to prove the air-blowing and vibrating supply seed tray structure could reduce the vibration frequency by 1.5 Hz and decrease the amplitude by 0.25 mm. The mathematical regression models between the inlet air pressure, vibration frequency, amplitude, and seeding performance indexes were established by orthogonal experiments. Through the optimization operation and bench tests, it was determined that when the inlet air pressure was 19.49 kPa, the vibration frequency was 9.00 Hz, and the amplitude was 2.65 mm, the eligible rate, replay rate, and hole rate could reach 93.56%, 3.35%, and 3.09%. The experimental results were generally consistent with the predicted values. The research confirmed that the air-blowing and vibrating supply seed tray could improve the eligible rate while reducing the vibration frequency and amplitude of the vacuum-vibration tray precision seeder. It also provided a necessary basis for precision seeding technology.

Keywords: air-blowing and vibrating, precision seeding, FLUENT, orthogonal experiment

DOI: 10.25165/j.ijabe.20221503.6873

Citation: Zhang Z Q, Chen J, Li Y M, Guan Z H, Liao C Q, Qiao X S. Design and experiment on the air-blowing and vibrating supply seed tray for precision seeders. Int J Agric & Biol Eng, 2022; 15(3): 115–121.

1 Introduction

Rice is a staple food for more than half of the world's population[1]. According to the statistical data, the planting area of super rice in China has exceeded 300 000 hm^2, and the yield has exceeded 15 000 kg/hm^2[2]. Hybrid rice has a greater ability to tiller than ordinary rice[3]. In order to fully release the planting potential of super rice and implement the precision agriculture strategy, the precision seedling cultivation of super rice puts forward higher requirements on seeding technology[4-6].

The seeding metering device is an essential device for a precision seeder. Foreign scholars have studied the working mechanism of the vacuum-type seeding metering device. Some vacuum-type seeding metering devices have been used for seeds with high spherical[7-9]. The super rice precision seeder is mainly based on the vacuum-vibration seeding metering device in China, which primarily uses the reciprocating vibration to excite the supply seed tray[10]. The suction plate uses negative pressure to suck seeds and positive pressure to discharge seeds. At present, this device is still in the research stage in China[11]. Zhao et al.[12,13] studied the law of the seed movement in the vibrating supply seed tray and predicted the distribution of seeds through the neural network, which provided a research basis for the adjustment of the vibration parameters of the vacuum plate seeder. Chen et al.[14,15] developed a vacuum-vibration precision seeder that basically meets the requirements of super rice precision seeding. However, using mechanical vibration to make the seeds in a discrete state easily led to uneven distribution. At the same time, the high-frequency vibration also caused the vibration of the whole machine, and the seeds fell off during the seeding process, which had a bad effect on the eligible rate. Therefore, improving the uniformity of the "boiling" movement of the seeds in the supply seed tray and reducing the vibration frequency and amplitude are of great significance for increasing the eligible rate of the vacuum-vibration seeder.

In this study, a method was proposed to make the seeds "boiling" in the supply seed tray under the combined effect of air blowing and vibration, and the air-blowing and vibrating supply seed tray structure were designed. Then, the optimal structural parameters of the supply seed tray were sought by fluid simulation. Orthogonal experiments were used to obtain the best working parameters under high seeding performance. Finally, Bench experiments were carried out to evaluate the seeding performance of the air-blowing and vibrating supply seed tray.

Received date: 2021-12-11 **Accepted date:** 2022-02-14

Biographies: Zhiqiao Zhang, MS candidate, research interest: agricultural machinery design and control technology, Email: zhangzhiqiao0921@gmail.com; **Yaoming Li**, PhD, Professor, research interest: modern agricultural machinery design and theoretical research, Email: ymli@ujs.edu.cn; **Zhuohuai Guan**, PhD, Research Assistant, research interest: monitoring and control technology for agricultural equipment, Email: guan_zh@Foxmail.com; **Caiqi Liao**, MS candidate, research interest: agricultural machinery design and control technology, Email: 2695026709@qq.com; **Xiangshan Qiao**, MS candidate, research interest: agricultural machinery design and control technology, Email: 2523024570@qq.com.

***Corresponding author: Jin Chen**, PhD, Professor, research interest: monitoring and control technology for agricultural equipment. College of Mechanical Engineering, Jiangsu University, Zhenjiang 212013, Jiangsu, China. Tel: +86-13052922858, Email: chenjinjd126@126.com.

2 Structure design of air-blowing and vibrating supply seed tray

2.1 Analysis of problems of vibrating supply seed tray

The structure of the vibrating supply seed tray is shown in Figure 1. The vibration excitation mechanism comprised a vibration motor, a crank connecting rod, a vibration spring, and a supply seed tray. The seeding process was as follows: the suction plate descended to the top of the vibrating seed tray and used the negative pressure to suck the seeds; then, the seeds were carried to the top of the seedling tray and blown into the seedling tray by positive pressure. Zhao et al.[16] investigated the influence of vibration parameters and seeds thickness on seeds movement and determined that the larger the vibration frequency and amplitude, the more easily the seeds would be dispersed, but the stability of seeds movement would decrease. Gong et al.[15] proved that the seeds did throwing movement in the seed tray when the amplitude was 4.09 mm and the vibration frequency was 10.90 Hz. However, when the vibration frequency exceeds 10 Hz, the springs at the top corner of the supply seed tray will drive the manipulator to vibrate, making the seeds fall off during the seed carrying process. At the same time, the uniformity and dispersion of the seeds are inadequate, leading to the decrease in the qualified rate.

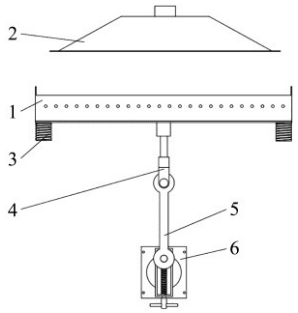

1. Vibrating seed tray 2. Suction plate 3. Spring 4. Y-shaped connector 5. Connecting rod 6. Vibration motor

Figure 1 Structure diagram of vibrating supply seed tray

2.2 Air-blowing and vibrating supply seed tray structure

Reducing the friction factor in the granules can increase their flowability and make the material move more evenly[17]. This paper proposed an air-blowing and vibrating supply seed tray structure. This structure used an excitation mechanism to excite the seed tray. It dispersed the air-blowing force through the holes at the bottom of the supply seed tray to improve seeds flowability and made the seeds do throwing motion in the supply seed tray. The seeds become quasi-fluid by "boiling" motion under the combined effect of vibration and air blowing.

In order to solve the problems of the vibrating supply seed tray, the structure of the air-blowing and vibrating supply seed tray was designed, as shown in Figure 2. The original excitation mechanism was retained, and the air-blowing mechanism was added. Add air-blowing chambers and air inlets at the bottom of the supply seed tray, and open four sets of 12×24 holes corresponding to the air-blowing chambers. The distribution of holes at the bottom of the supply seed tray is shown in Figure 3. The air-blowing chambers were connected to the bottom of the supply seed tray by bolts 5 mm in diameter, and the airflow generated by the air pump was evenly dispersed to the holes at the bottom of the supply seed tray so that the seeds could obtain evenly blowing force. Since the inlet air pressure, the diameter of the holes at the bottom of the supply seed tray, and the number of air inlets directly impacted the airflow velocity of the holes at the bottom of the supply seed tray. The digital analysis and design of the above parameters would be carried out to determine the structural parameters of the seed supply tray.

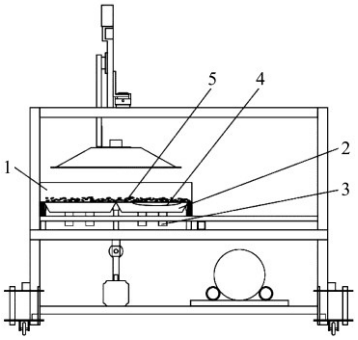

1. Supply seed tray 2. Air chamber 3. Air inlet 4. Holes at the bottom of the supply seed tray 5. Seeds

Figure 2 Front view of the air-blowing and vibrating supply seed tray

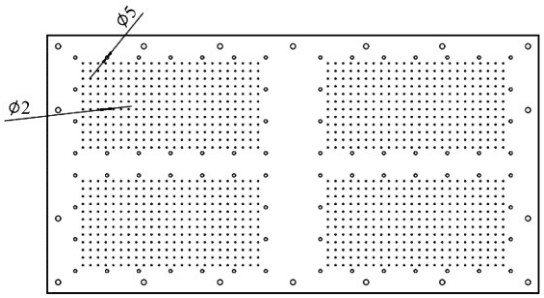

Figure 3 Distribution of holes at bottom of the supply seed tray

3 Optimized design of structure parameters

3.1 Build airflow field model and meshing

FLUENT can be used to analyze the airflow field of the air-blowing and vibrating supply seed tray[18,19]. A quarter of the fluid area was selected for analysis due to the limitation of the computer performance. The airflow field model of the air-blowing and vibrating supply seed tray was established by UG as shown in Figure 4. The size of the air chamber was 367.5 mm× 187.5 mm, the height was 50 mm, the draft angle was 30°, the size of the supply seed tray air chamber was 380 mm×195 mm×60 mm, the thickness of the bottom surface of the supply seed tray was 5 mm, and the diameter of the air inlets was 40 mm, height was 60 mm.

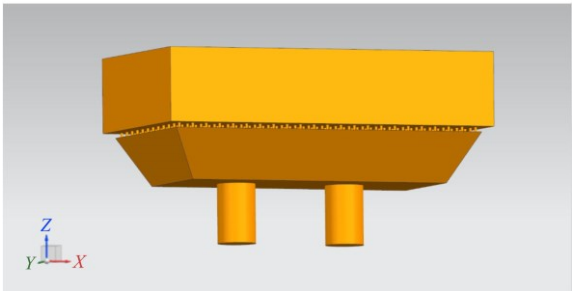

Figure 4 Airflow field model of air-blowing and vibrating supply seed tray

The airflow field of the air-blowing and vibrating supply seed tray was meshed by ICEM CFD[20]. Considering the holes were small at the bottom of the supply seed tray, the tetrahedral mesh was used. In order to obtain the accurate airflow field parameters of the holes at the bottom of the supply seed tray, the local mesh was refined. The grid diagram of the airflow field is shown in Figure 5. The results indicated that the quality of the grids

divided by this method was greater than 0.35, of which the proportion of more than 0.9 was 80.2%, and the number of grids was 240 874. This method could accelerate the calculation speed while guaranteeing accuracy.

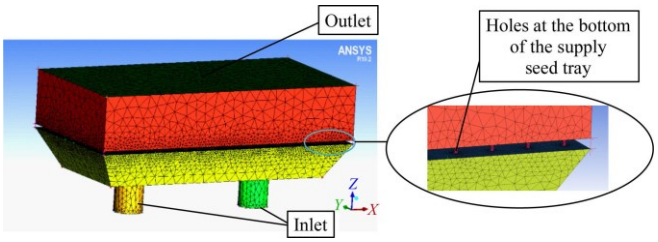

Figure 5 Airflow field grid diagram of air-blowing and vibrating supply seed tray

3.2 Numerical simulation of airflow field

The effects of different inlet air pressures, the number of air inlets, and the diameter of the holes at the bottom of the supply seed tray on the airflow field were analyzed to set the parameter ranges for structural parameters optimization simulation.

3.2.1 Inlet air pressure

The hole diameter at the bottom of the seed tray was 2 mm, and the number of air inlets was 2. It was found in the preliminary experiment that the seeds were dispersed when the inlet air pressure was greater than 16 kPa. The inlet air pressure values were 16 kPa, 20 kPa, and 22 kPa for simulation. The post-processing software CFD-post was used to extract the airflow field parameters at the holes at the bottom of the supply seed tray, as shown in Table 1. As the inlet air pressure increased, the airflow velocity at the holes at the bottom of the supply seed tray had a marked rise, and the air-blowing force increased gradually. Hence, the greater the inlet air pressure was, the higher the dispersion of seeds became.

Table 1 Influences of different inlet air pressure on airflow field parameters

Airflow field parameter	Inlet air pressure/kPa		
	16	20	22
V_r/m·s^{-1}	154.5-174.6	149.7-182.7	162.0-191.7
V_a/m·s^{-1}	163.2	169.7	173.2
P_r/kPa	318.3-1511.0	397.8-1436.9	401.2-2403.0
P_a/kPa	743.5	795.5	821.6
F_r/N	0.00078-0.00095	0.00075-0.0010	0.00084-0.00115
F_a/N	0.00082	0.00084	0.00093

Note: V_r represents the range of velocity; V_a represents the average of velocity; P_r represents the pressure range of the holes at the bottom of the supply seed tray; P_a represents the pressure average of the holes at the bottom of the supply seed tray; F_r represents the force range in Z direction; F_a represents the average of the force in the Z direction.

3.2.2 Number of the air inlet

The diameter of the holes at the bottom of the seed tray was set to 2 mm. The inlet air pressure was 16 kPa. The diameter of the air inlet was 40 mm. Considering the interference between the bottom of the seed tray and the original excitation structure, the height of the air inlet was fixed at 50 mm. The number of air inlets was chosen to be 2 (uniformly distributed at the bottom of the air chamber), 3 (uniformly distributed at the middle of the bottom of the air chamber), and 4 (distributed at the top corner of the bottom of the seed chamber) for simulation. The velocity cloud diagram of the holes at the bottom of the supply seed tray is shown in Figure 6. The airflow field parameters of the holes at the bottom of the supply seed tray are listed in Table 2. The results indicated that when the number of air inlets increased, there were only slight changes in the airflow velocity of the holes at the bottom of the supply seed tray and the force in the Z-direction. Still, the force range had a gradual decline, indicating that the airflow of the bottom holes of the supply seed tray became uniform. So, the number of air inlets had an important effect on the uniformity of airflow distribution.

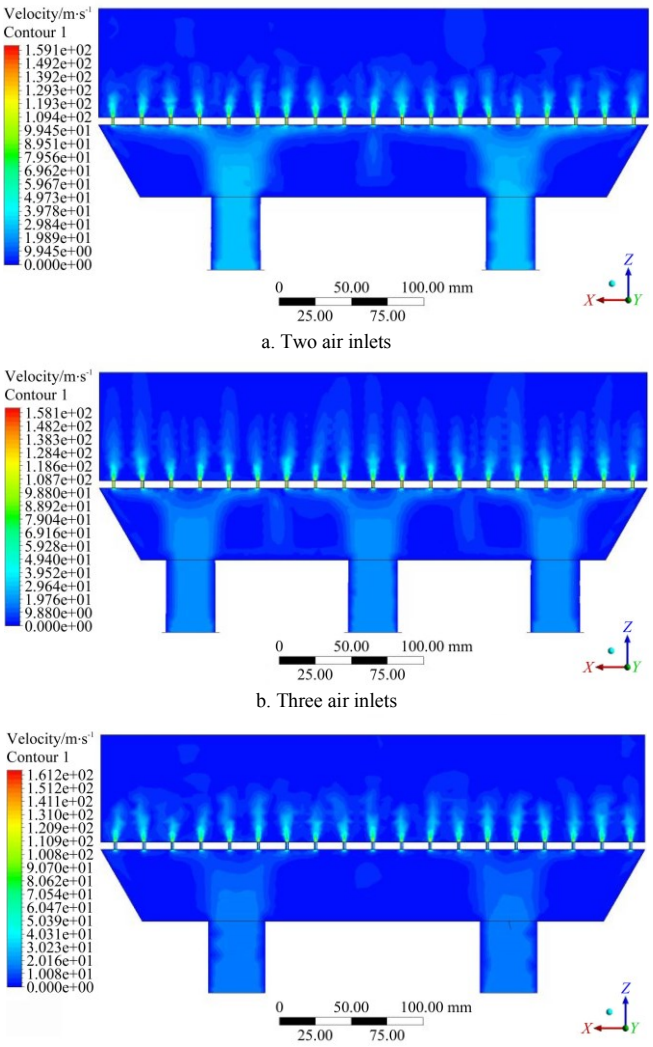

Figure 6 Velocity distribution of the different number of air inlets

Table 2 Influences of the different numbers of air inlets on airflow field parameters

Airflow field Parameter	Number of air inlets		
	2	3	4
V_r/m·s^{-1}	138.2-156.1	139.1-154.7	145.3-157.6
V_a/m·s^{-1}	145.1	143.2	145.1
P_r/kPa	312.3-1851.0	244.5-1528.0	324.0-1975.0
P_a/kPa	674.5	693.5	724.0
F_r/N	0.00057-0.00118	0.00061-0.00081	0.00063-0.0074
F_a/N	0.00071	0.00074	0.00069

3.2.3 Diameter of the holes at the bottom of the supply seed tray

The diameter of the holes at the bottom of the supply seed tray is related to the three-axis size of the super rice. The empirical formula was adopted to determine the hole diameter range at the bottom of the supply seed tray as: 1.59-2.34 mm, and 1.7 mm, 2.0 mm, and 2.3 mm were selected for simulation. There were two air inlets, and the inlet air pressure was 16 kPa. The results

are shown in Table 3. The data suggested that when the hole diameter at the bottom of the supply seed tray decreased, the airflow velocity had a steady rise, but the pressure range increased rapidly. It indicated that the airflow uniformity was gradually deteriorating. The average of the force in Z direction was small. When the uniformity of airflow field becomes worse, the correlation between the average of the force in Z direction and air blowing effect evaluation is weakened. Hence, the airflow velocity can be used to evaluate air-blowing effect.

Table 3 Influence of the different hole diameters at the bottom of the supply seed tray

Airflow field parameter	Diameter of the holes at the bottom of the supply seed tray/mm		
	1.7	2.0	2.3
V_r/m·s^{-1}	141.3-153.9	141.7-156.3	140.5-157.5
V_a/m·s^{-1}	147.5	143.2	138.6
P_r/kPa	341.9-2519.0	336.5-1978.0	270.0-1651.0
P_a/kPa	795.3	693.8	754.1
F_r/N	0.00063-0.00085	0.00059-0.00078	0.00054-0.00084
F_a/N	0.000676	0.00074	0.00069

3.3 Optimization simulation of structural parameters

The ranges of the parameters were set according to numerical simulation results of the airflow field. Taking the maximum airflow velocity of the holes at the bottom of the supply seed tray as the response value, FLUENT was used to numerically simulate the airflow field of the air-blowing and vibrating supply seed tray. Orthogonal tests with three factors and three levels were used to determine the primary and secondary factors affecting the airflow velocity of the holes at the bottom of the supply seed tray and the optimal combination. The factor level table is listed in Table 4.

Table 4 Orthogonal table of three factors and three levels

Level	Factor		
	A/kPa	B/PCS	C/mm
1	16	2	1.7
2	20	3	2.0
3	22	4	2.3

Note: A represents the inlet air pressure; B represents the number of air inlets; C represents the diameter of the holes at the bottom of the supply seed tray.

The maximum airflow velocity of the holes at the bottom of the supply seed tray could be obtained by simulation. The range analysis method was used to calculate the range of each group of factors to determine the primary and secondary order of the influence of each factor on the maximum airflow velocity and obtain the optimal plan. Table 5 shows the relationship between the range of each factor: R_A>R_C>R_B. The primary and secondary order of the factors affecting the maximum airflow velocity of the holes at the bottom of the supply seed tray was the inlet air pressure, the diameter of the holes at the bottom of the supply seed tray, and the number of air inlets. When the number of air inlets was selected at level three, the installation area was limited, so factor B selected level 1 as the best level. The optimal solution was: A3B1C2. The inlet air pressure was 22 kPa, the hole diameter at the bottom of the seed tray was 2 mm, and the number of air inlets was 2.

3.4 Verification experiments

The wind speed measuring instrument installation requires a hole in the side plate of the seed tray. To avoid damaging the structure of the supply seed tray on the vacuum-vibration precision seeder, a flow velocity test platform was developed to measure the

Table 5 Simulation results of the influence of three factors on the maximum airflow velocity

Number	Factor			Maximum airflow velocity/m·s^{-1}
	A/kPa	B/PCS	C/mm	
1	16	2	1.7	147.25
2	16	3	2.0	150.58
3	16	4	2.3	151.30
4	20	2	2.0	167.32
5	20	3	2.3	168.94
6	20	4	1.7	166.04
7	22	2	2.3	174.92
8	22	3	1.7	174.29
9	22	4	2.0	177.71
K_1	449.14	489.50	487.59	
K_2	502.30	493.82	495.62	
K_3	526.94	495.06	495.18	
k_1	149.71	163.17	162.53	
k_2	167.44	164.61	165.21	
k_3	175.65	165.02	165.06	
Range R	77.80	5.55	8.03	
Primary and secondary factor			A>C>B	
Best plan		A3B3C2		

flow velocity of the holes at the bottom of the supply seed tray. It was used to verify the reliability of the simulation results of the airflow field. As shown in Figure 7, the side plate of the supply seed tray had five sets of holes for installing the wind speed measuring instrument. The wind speed measuring instrument was mounted directly above the holes at the bottom of the supply seed tray, 30 mm away from the panel, to measure the airflow velocity of the holes at the bottom of the supply seed tray. The inlet air pressure was set to 22 kPa, the diameter of the holes at the bottom of the supply seed tray was 2 mm, and the number of air inlets was 2. The wind speed was measured three times, and the average values were recorded. The test result is shown in Figure 8.

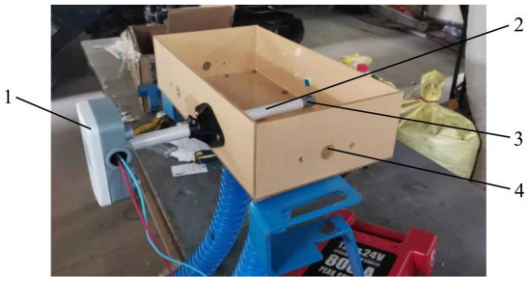

1. Screen of the wind speed measuring instrument 2. Wind speed probe rod
3. Wind speed measuring probe 4. Mounting hole

Figure 7 Flow velocity test platform

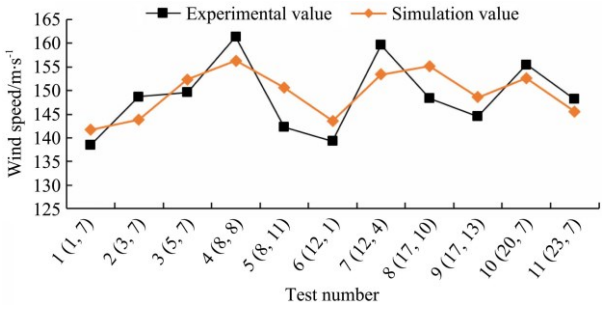

Note: a(b, c): a represents the test sequence number, b represents the row number of the selection hole, and c represents the column number of the selection hole.

Figure 8 Comparison of simulation and experimental data

The results revealed that the airflow velocity of the holes at the bottom of the supply seed tray obtained by simulation only had a

slight difference from the experimental value, which indicated that the digital design of the structural parameters of the air-blowing and vibrating supply seed tray was feasible by FLUENT.

4 Bench experiments and results analysis

4.1 Air-blowing and vibrating supply seed tray test platform

The air-blowing and vibrating supply seed tray test platform was built based on the vacuum-vibration precision seeder, as shown in Figure 9. The upper part of the air chamber was connected with the supply seed tray, and the lower part was connected with the air intake pipe. The manipulator was set above the supply seed tray to cooperate with the assembly line for sowing.

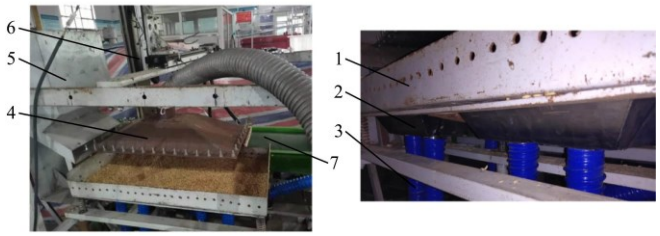

1. Supply seed tray 2. Air chamber 3. Air intake pipe 4. Suction plate
5. Seed box 6. Manipulator 7. Assembly line

Figure 9 Air-blowing and vibrating supply seed tray test platform

Changyou No. 3 super rice was used as the test material. The seeds were soaked and dried before experiments. The seedling tray adopted a potted blanket seedling tray with 31 rows×14 rows of holes, with 434 holes. The seedling tray was put on the rigid tray. The manipulator cooperated with the assembly line to carry out the seeding test. The test site is shown in Figure 10. To observe the seeding performance, covering topsoil and sweeping topsoil were not performed during the experiment.

Figure 10 Seeding process of precision seeder

4.2 Comparative experiment

By changing the vibration frequency and amplitude to compare the eligible rate by single vibrating supply seed tray and air-blowing and vibrating supply seed tray, the superiority of air-blowing and vibrating supply seed tray was verified. When the air pump was turned off and the inlet air pressure was 0 Pa, it was regarded as the single vibrating supply seed tray for seeding. When the air pump was turned on and the inlet air pressure was 20 kPa, it was regarded as the air-blowing and vibrating supply seed tray for seeding. In the following section, the pressure values of 0 Pa and 20 kPa at the inlet of the supply seed tray will be used to indicate the seeding situation with a single vibration supply seed tray and an air-blowing and vibrating supply seed tray.

4.2.1 Vibration frequency

In order to compare the vibration frequency of the single vibrating supply seed tray and the air-blowing and vibrating supply seed tray when the eligible rate reaches best, the amplitude was set to 3.5 mm, and the vibration frequency of 8-12 Hz was selected with 0.5 Hz as a step. Each group test was carried out five times, and the average value was taken as the final eligible rate. The comparative experiment results are shown in Figure 11. The results showed that when the vibration frequency was 9 Hz and the inlet air pressure was 20 kPa, the eligible rate was more than 95% at a higher level. When the vibration frequency was 10.5 Hz and the inlet air pressure was 0 Pa, the eligible rate was more than 95%. Therefore, the air-blowing and vibrating supply seed tray could reduce the vibration frequency by 1.5 Hz.

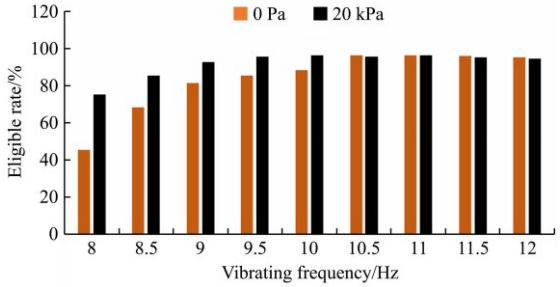

Figure 11 Comparison test results under different vibration frequencies

4.2.2 Amplitude

To compare the amplitude of the single vibrating supply seed tray and the air-blowing and vibrating supply seed tray when the eligible rate reaches better, the vibration frequency was fixed at 9.5 Hz, and the amplitude range was selected: 1.5-3.5 mm, with 0.25 mm as a step. The group test was conducted five times, and the average value was taken as the final eligible rate. The results are shown in Figure 12. The results showed that when the amplitude was 3 mm and the inlet air pressure was 20 kPa, the eligible rate was more than 93% at a higher level. When the amplitude was 2.75 mm and the inlet air pressure was 0 Pa, the eligible rate was more than 94%. Therefore, the air-blowing and vibrating supply seed tray could reduce the amplitude by 0.25 mm.

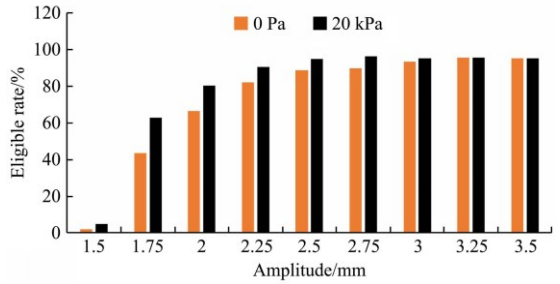

Figure 12 Comparative experiment results under different amplitudes

4.3 Orthogonal experiment

4.3.1 Orthogonal Experiment method

The single factor analysis could determine that the vibration frequency range was: 7-11 Hz, the amplitude range was: 1.5-3.5 mm, and the range of the inlet air pressure was: 17-22 kPa. With reference to the national standard, the eligible rate, replay rate, and hole rate were used as evaluation indexes. The mathematical regression model between inlet air pressure, vibration frequency, amplitude, and sowing performance indexes were established by the quadratic regression orthogonal rotational combination test. The test factor level coding table is listed in Table 6, and the experimental design plan and response value results are shown in Table 7. Each group of experiments was repeated five times, and the average value was recorded. Seeding performance evaluation index expressions are given by

$$Y_1 = \frac{n_1}{N} \times 100\% \quad (1)$$

$$Y_2 = \frac{n_2}{N} \times 100\% \quad (2)$$

$$Y_3 = \frac{n_3}{N} \times 100\% \quad (3)$$

where, Y_1 represents eligible rate; Y_2 represents replay rate; Y_3 represents hole rate; n_1 represents the number of holes for one or two seeds; n_2 represents the number of holes for more than two seeds; n_3 represents the number of no seed holes; N represents the total number of holes in the seedling tray, and the value of N is 434.

Table 6 Coding of test factors and levels

Level	Factor		
	Inlet air pressure X_1/kPa	Vibration frequency X_2/Hz	Amplitude X_3/mm
1.682	22.00	11.00	3.50
1	20.99	10.19	3.09
0	19.50	9.00	2.50
–1	18.01	7.81	1.91
–1.682	17.00	7.00	1.50

4.3.2 Orthogonal test results

Quadratic polynomial regression models between the experimental factors and the super rice seeding performance indexes were established by the data processing software Design Expert V8.0.6.1. The regression model equations were given by

$$Y_1 = -260.07 + 27.25X_1 + 10.94X_2 + 34.960X_3 - 0.16X_1X_2 - 1.68X_1X_3 + 1.26X_2X_3 - 0.56X_1^2 - 0.62X_2^2 - 2.89X_3^2 \quad (4)$$

$$Y_2 = 294.92 - 22.37X_1 - 8.05X_2 - 31.79X_3 + 0.20X_1X_2 + 1.64X_1X_3 - 1.73X_2X_3 + 0.42X_1^2 + 0.48X_2^2 + 3.38X_3^2 \quad (5)$$

$$Y_3 = 65.16 - 4.88X_1 - 2.89X_2 - 3.16X_3 + 0.04X_1X_2 + 0.04X_1X_3 + 0.48X_2X_3 + 0.14X_1^2 + 0.14X_2^2 - 0.49X_3^2 \quad (6)$$

Table 8 provides the results of the regression model analysis of variance and significance test. The results indicated that the fitting of the eligible rate, replay rate, and hole rate model was extremely significant ($p<0.01$). The regression equation was not significantly out of fit, which fit well with the actual situation.

Table 7 Experiment design and response values

No.	Factor level			Response value		
	X_1/kPa	X_2/Hz	X_3/mm	Y_1/%	Y_2/%	Y_3/%
1	1	1	1	89.4	7.1	3.5
2	1	1	–1	95.1	1.8	3.1
3	1	–1	1	88.9	7.8	3.3
4	1	–1	–1	90.8	7.4	1.8
5	–1	1	1	92.8	3.6	3.6
6	–1	1	–1	89.7	7.6	2.7
7	–1	–1	1	93.0	2.9	4.1
8	–1	–1	–1	91.6	4.8	3.6
9	1.682	0	0	90.4	5.5	4.1
10	–1.682	0	0	90.6	6.2	3.2
11	0	1.682	0	89.4	6.8	3.8
12	0	–1.682	0	93.6	3.5	2.9
13	0	0	1.682	89.5	8.7	1.8
14	0	0	–1.682	92.7	4.5	2.8
15	0	0	0	95.2	2.1	2.7
16	0	0	0	94.6	2.2	3.2
17	0	0	0	95.3	1.4	3.3
18	0	0	0	95.2	2.1	2.7
19	0	0	0	92.7	4.2	3.1
20	0	0	0	93.5	4.7	1.8
21	0	0	0	90.8	5.6	3.6
22	0	0	0	96.1	1.0	2.9
23	0	0	0	96.0	0.9	3.1

Note: X_1 represents inlet air pressure; X_2 represents vibration frequency; X_3 represents amplitude.

Table 8 Variance analysis of the orthogonal test results

Source	Eligible rate				Replay rate				Hole rate			
	s	df	F	p	s	df	F	p	s	df	F	p
Model	88.78	9	3.22	0.0028	84.82	9	3.22	<0.0001	6.87	9	2.94	0.0038
X_1	0.97	1	0.33	0.0057	0.14	1	0.047	0.0083	1.84	1	7.08	0.0196
X_2	1.52	1	0.52	<0.0001	0.55	1	0.19	<0.0001	0.24	1	0.93	0.0354
X_3	4.78	1	1.64	0.0096	11.01	1	3.76	0.0745	1.28	1	4.92	0.0449
X_1X_2	0.66	1	0.23	0.6413	0.98	1	0.33	0.5728	0.031	1	0.12	0.7344
X_1X_3	17.70	1	6.09	0.0283	16.82	1	5.74	0.0323	0.011	1	0.043	0.8385
X_2X_3	6.30	1	2.17	0.1648	12.01	1	4.10	0.0640	0.91	1	3.50	0.0839
X_1^2	24.15	1	8.31	0.0128	13.75	1	4.69	0.0494	1.45	1	5.59	0.0343
X_2^2	12.28	1	4.22	0.0605	7.41	1	2.53	0.1358	0.61	1	2.36	0.1487
X_3^2	16.55	1	5.69	0.0329	22.71	1	7.75	0.0155	0.49	1	1.87	0.1951
Residual	37.80	13			38.53	13			3.38	13		
Lack of fit	14.23	5	0.97	0.4913	14.76	5	1.01	0.4688	0.68	5	0.4	0.8335
Pure error	23.57	8			23.32	8			2.70	8		
Cor total	122.01	22			122.89	22			10.26	22		

Note: s represents sum of squares; df represents degree of freedom; F represents F value; p represents the result of significance test, and p value of the model is less than 0.05 indicate model terms are significant.

Under the premise that the regression model was significant and the lack-of-fit item was not significant, the insignificant regression items were eliminated. The regression equations of the eligible rate, replay rate, and cavity rate were refitted. After testing, in the eligible rate regression equation, the interaction terms between the inlet air pressure and the vibration frequency and the interaction terms between the vibration frequency and amplitude had no significant influence on the eligible rate. The replay rate regression equation indicated that the interaction terms between the inlet air pressure and the vibration frequency and the quadratic term of the vibration frequency had no significant influence on the replay rate. According to the hole rate regression equation, the interaction terms between the inlet air pressure and the vibration frequency, the interaction terms between the inlet air pressure and amplitude, and the quadratic term of vibration frequency and amplitude had no significant influence on the hole rate. Therefore, the regression equations after refitting were given by

$$Y_1 = -259.77 + 25.79X_1 - 10.91X_2 + 46.26X_3 - 1.68X_1X_3 - 0.56X_1^2 - 0.62X_2^2 - 2.89X_3^2 \quad (7)$$

$$Y_2 = 220.58 - 20.50X_1 + 4.50X_2 - 31.73X_3 + 1.64X_1X_3 - 1.73X_2X_3 + 0.42X_1^2 + 3.37X_3^2 \quad (8)$$

$$Y_3 = 61.12 - 5.01X_1 - 1.08X_2 - 4.81X_3 + 0.48X_2X_3 + 0.14X_1^2 \quad (9)$$

The equation's regression coefficients suggested that the

primary and secondary order of the effects of each factor on the eligible rate and replay rate were in the following order: amplitude, vibration frequency, and inlet air pressure. The primary and secondary order of the influence of each factor on the hole rate was inlet air pressure, amplitude, and vibration frequency.

4.4 Optimization of working parameters

Various factors and the interaction between the factors had a significant impact on the performance of the precision seeder. In order to obtain the best seeding operation parameters, the inlet air pressure, vibration frequency, and amplitude need to be optimized. In actual planting operations, the eligible rate Y_1 should be as large as possible under the condition of meeting the agronomic requirements. The hole rate Y_3 should be as low as possible. The requirement for the replay rate Y_2 was relatively low. The parameter optimization conditions were given by

$$\begin{cases} \max \quad Y_1 \\ \min \quad Y_3 \\ 17 \le X_1 \le 22 \\ 7 \le X_2 \le 11 \\ 1.5 \le X_3 \le 3.5 \end{cases} \tag{10}$$

The optimized working parameter combination was as follows: the inlet air pressure was 19.49 kPa, the vibration frequency was 9.00 Hz, and the amplitude was 2.65 mm. In this situation, predictive values of the eligible rate, the replay rate, and the hole rate were 94.22%, 3.27%, and 2.86%.

Testing on the air-blowing and vibrating supply seed tray test platform to verify the reliability of the optimal working parameter combination. The inlet air pressure was 19.49 kPa. The vibration frequency was 9.00 Hz. The amplitude was 2.65 mm. The measurements were repeated five times, and the averages were taken as the seeding performance indexes. The results showed that the eligible rate was 93.56%, the replay rate was 3.35%, and the hole rate was 3.09%. It suggested that the optimized parameter combination could more effectively improve the seeding performance of the air-blowing and vibration supply seed tray for precision seeder.

5 Conclusions

1) A method was proposed to make the seeds “boiling” under the combined effect of air blowing and vibration. The structure of the air-blowing and vibrating supply seed tray was designed. FLUENT was used to analyze the air chamber in the supply seed tray to determine that the airflow velocity of the holes at the bottom of the supply seed tray was the highest when the inlet pressure was 22 kPa, the number of air inlets was 2, and the diameter of the holes at the bottom of the supply seed tray was 2 mm.

2) With the comparison test between the air-blowing and vibrating supply seed tray and the vibrating supply seed tray, it was clear that the air-blowing and vibrating supply seed tray could reduce the vibration frequency by 1.5 Hz and the amplitude by 0.25 mm.

3) When the inlet air pressure was 19.49 kPa, and the vibration frequency was 9.00 Hz, and the amplitude was 2.65 mm, the air-blowing and vibrating supply seed tray had the best seeding performance. The values of the eligible rate, replay rate, and hole rate could reach 93.56%, 3.35%, and 3.09%.

This study proposed a method for designing the supply seed tray structure from the perspective of the force on the seeds. This new structure can achieve a high eligible rate while reducing the vibration of the whole machine. It also provides an essential basis for further research on the setting of the working parameters of the precision seeder.

Acknowledgements

This study was financially supported by the National Natural Science Foundation of China (Grant No. 31871528), and Key Laboratory of Modern Agricultural Equipment and Technology (Jiangsu University), Ministry of Education (MAET202106).

[References]

[1] Fukagawa N K, Ziska L H. Rice: Importance for global nutrition. Journal of Nutritional Science and Vitaminology, 2019; 65: S2–S3.

[2] Liu Z, You L L, Wang S L, Fu M. Talking about the current situation and development trend of rice seedling raising equipment in my country. Agricultural Development and Equipment, 2020; 11: 26–27. (in Chinese)

[3] Yang Z Y, Li N, Ma J, Sun Y J, Xu H. High-yielding traits of heavy panicle varieties under triangle planting geometry: A new plant spatial configuration for hybrid rice in China. Field Crops Research, 2014; 168: 135–147.

[4] Yuan L P. Progress in breeding of super hybrid rice. Journal of Agronomy, 2018; 8(1): 71–73. (in Chinese).

[5] Bao S S. Current situation and suggestions of my country's grain planting structure adjustment under the background of supply-side reform. Rural Economy and Science-Technology, 2019; 303(14): 207–208. (in Chinese)

[6] Song J N, Zhuang N S, Wang L C, Liu X W, Wei W J. The development tendency of Chinese rice planting mechanization in the 21st Century. Journal of China Agricultural University, 2000; 5(2): 30–33. (in Chinese)

[7] Lauriano S M, de Sousa S F G, Dias P P, Correia T P S, Silva P R A. Seeder performance under different pressures of vacuum and fuel consumption to soybean seeds. Bioscience Journal, 2017; 33(5): 1119–1125.

[8] Hossein B. Modeling and evaluation of a vacuum - cylinder precision seeder for chickpea seeds. Agricultural Engineering International: CIGR Journal, 2019; 21(4): 75–82.

[9] Arzu Y, Adnan D. Optimisation of the seed spacing uniformity performance of a vacuum-type precision seeder using response surface methodology. Biosystems Engineering, 2007; 97(3): 347–356.

[10] Gong Z Q, Chen J, Li Y M, Wang C J, Hang C. Study on Field Seedling Raising Vacuum-vibration Tray Precision Seeder's Horizontal Adjustment Mechanism. Advances in Design Technology, 2012; (215–216): 142. doi: 10.4028/www.scientific.net/AMM.215-216.142

[11] Li Z H, Ma X, Li X C, Li L T, Li H W, Yuan Z C. Research Progress of Rice Transplanting Mechanization. Transactions of the CSAM, 2018; 49(5): 1–20. (in Chinese)

[12] Zhao Z, Jin M Z, Tian C J, Yang S X. Prediction of seed distribution in rectangular vibrating tray using grey model and artificial neural network. Biosystems Engineering, 2018; 175: 194–205.

[13] Zhao Z, Tian C J, Wu Y F, Huang H D. Dynamic simulation of seed pick-up process and parameter optimization on vacuum plate seeder for rice. Transactions of the CSAE, 2018; 34(7): 38–44. (in Chinese).

[14] Chen J, Gong Z, Li Y, Li J, Xu Y. Experimental study on nursing seedlings of super rice precision seeder device. Transactions of the CSAM, 2015; 46(1): 73–78. (in Chinese)

[15] Gong Z, Chen J, Li Y, Li J. Seed force in airflow field of vacuum tray precision seeder device during suction process of seeds. Transactions of the CSAM, 2014; 45(6): 92–97, 117. (in Chinese)

[16] Zhao Z, Wu Y F, Yin J J, Tang Z. Monitoring method of rice seeds mass in vibrating tray for vacuum-panel precision seeder. Computers & Electronics in Agriculture, 2015; 114: 25–31.

[17] Hu S, Siebenmorgen T J. Effect of rice cultivar, type, form, and moisture content on the angle of repose. Applied Engineering in Agriculture, 2019; 35(4): 561–568.

[18] Xing H, Zang Y, Wang Z M, Luo X W. Design and parameter optimization of rice pneumatic seeding metering device with adjustable seeding rate. Transactions of the CSAE, 2019; 35(4): 20–28. (in Chinese)

[19] Deng W, Zhang R R, Xu G, Li L L. The influences of the nozzle throat length and the orifice grooving degree on internal flow field for a multi-entry fan nozzle based on FLUENT. Engineering, 2019; 11(11): 777–790.

[20] Jain S, Patil R S. Numerical simulation of novel nozzle intake manifold. Journal of Physics: Conference Series, 2019; 1276(1): 012037. doi: 10.1088/1742-6596/1276/1/012037.